

Kinematics of Top Quark Final States: A Snowmass White Paper

ANDREAS JUNG^a, MARKUS SCHULZE^b, AND JESSIE SHELTON^c

^a *Fermilab, DAB5 - MS 357,
P.O. Box 500, Batavia, IL, 60510, USA*

^b *High Energy Physics Division,
Argonne National Laboratory, Argonne, IL 60439, USA*

^c *Center for the Fundamental Laws of Nature,
Harvard University, Cambridge, MA 02138, USA*

with contributions from

T. Schwarz, S. Berge, S. Westhoff, and V. Coco (for the LHCb Collaboration)

Abstract

This is the summary report of the Top Quark Kinematics working group prepared for Snowmass 2013. We study theoretical predictions for top pair differential distributions, in both boosted and un-boosted regimes, and present an overview of uncertainties and prospects for top spin correlations. We study the prospects for measuring the inclusive SM top pair production asymmetry A_{FC} at LHC 14 as a function of systematic error, and show that some improvement over current systematic uncertainties, as customarily handled, is required for observing a SM-size asymmetry. Cuts on top pair invariant mass and rapidity do not substantially alter this conclusion. We summarize the conclusions of contributed studies on alternate LHC measurements of the $t\bar{t}$ production asymmetry, in $t\bar{t}$ +jet final states and in forward top production at LHCb, both of which show good prospects for observing SM-size asymmetries in 50 fb^{-1} of data at LHC14.

1 Introduction

The top quark, the heaviest known elementary particle, has a lifetime significantly shorter than the time scale required for hadronization. Due to this short lifetime, bare top quark properties can be observed by measuring the kinematics of the top's decay products. Top pair production events are important both as a signal in their own right and as a background to physics beyond the Standard Model (BSM). A detailed understanding of top quark kinematics is necessary in order to observe potential effects of BSM physics in top pair production, or to predict top backgrounds for signals of direct BSM production.

This white paper collects the results of the Top Kinematics working group prepared for Snowmass 2013. It contains results of dedicated studies performed by the coordinators of the working group (A. Jung, M. Schulze, and J. Shelton), with additional input from T. Schwarz, and summarizes the conclusions from contributed studies by S. Westhoff and S. Berge and by the LHCb collaboration, which appear in full elsewhere [1, 2].

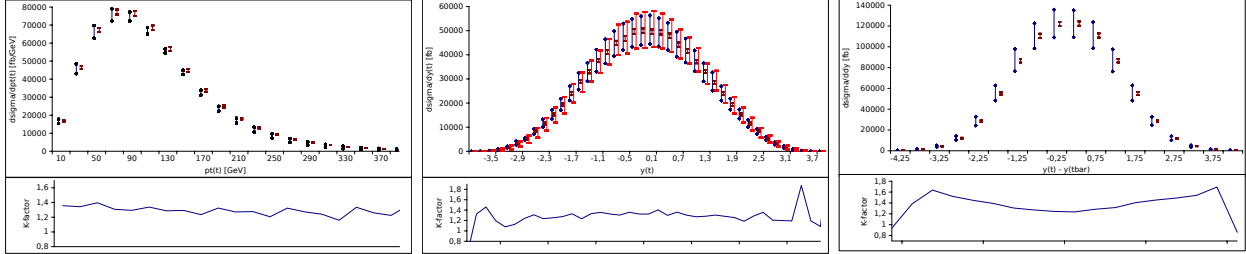


Figure 1: NLO QCD predictions [3] for transverse momentum, rapidity and rapidity difference at the 14 TeV LHC. Blue error bars correspond to scale variation by a factor of two around m_t . Dark red error bands correspond to variation of different MSTW pdf error sets. The additional band in the y_t distribution shows the variation with NN pdf error sets.

Section 2 begins with a study of theoretical uncertainties on basic kinematic distributions in top quark pair production at the 14 and 33 TeV LHC, and in Section 3 the same uncertainties are considered for the high p_T tails of the top quark production cross-sections. Section 4 summarizes results on top quark spin correlations. In Section 5, the observability of the inclusive SM top quark charge asymmetry at the 14 TeV LHC is studied as a function of experimental systematic uncertainties. Section 6 summarizes studies for alternate measurements of the top quark production asymmetry, both in $t\bar{t}$ +jet final states at LHC 14 and LHC 33 and inclusively at LHCb.

2 Basic kinematic distributions

In this section we summarize theoretical uncertainty estimates for top quark pair production at the 14 TeV and 33 TeV LHC. The results are obtained from the publicly available program MCFM [3] at next-to-leading order (NLO) QCD. Uncertainties are estimated by varying renormalization and factorization scales as well as by using different parton distribution functions and their error sets. We assume stable top quarks and consider the total $t\bar{t}$ cross section and distributions in the top quark transverse momentum, its rapidity and the difference of top and anti-top quark rapidity. The aim of this study is to provide error estimates that can be used to extrapolate uncertainties on more complicated observables that involve the top quark decay products. Explicit NLO predictions for top-quark pair production and decay have been presented in Refs. [4, 5, 6, 7, 8, 9, 10, 11, 12, 13, 14].

The total NLO QCD $t\bar{t}$ cross section at the 14 TeV LHC is 845 pb. Next-to-leading order QCD corrections reduce the scale dependence by more than a factor of two and enhance the total cross section by 30%. The residual scale uncertainty amounts to about 12% when varied by a factor of two around $m_t = 173$ GeV. Variations of 40 error sets of the MSTW pdf set [15] amount to shifts of about 2 % of the total cross section at leading and next-to-leading order QCD. Using the different pdf fits of the NN group [16], we find a total cross section with a central value deviating by less than one % from the MSTW result. However, the error bars of NN pdfs are significantly larger than those in the MSTW pdf sets, amounting to about 8 %.

In Fig. 2 we show the kinematic distributions of top quark transverse momentum, rapidity

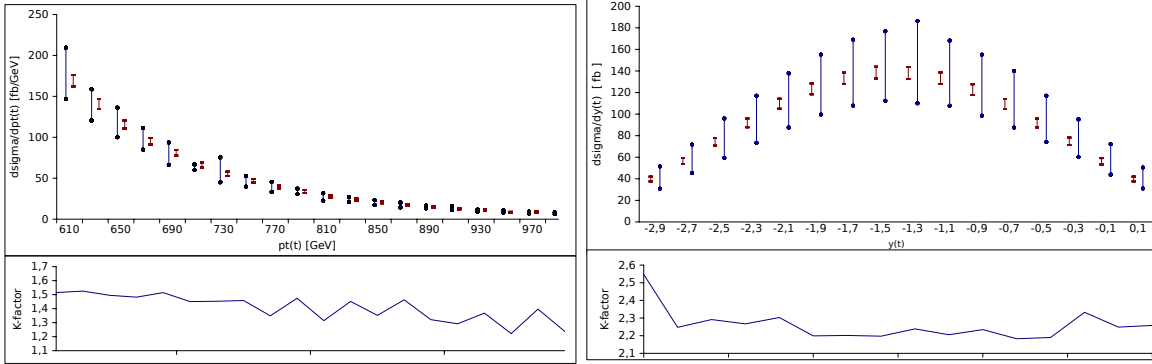


Figure 2: NLO QCD predictions [3] for top quark transverse momentum and rapidity with $p_{\perp}^t \geq 600$ GeV at the 14 TeV LHC.

and the rapidity difference between top and anti-top quark at NLO QCD. The transverse momentum distribution can be predicted with an approximate uncertainty of 15-20%. In contrast to the LO predictions, which have an almost constant error over the entire p_{\perp} range, NLO effects show largest scale dependence close to threshold and smaller scale dependence at higher energies. Variations from different MSTW pdf error sets amount to about a 2-8% spread in the p_{\perp} bins. The rapidity distribution of a top quark has a residual scale dependence of up to 20% in the central region. In Fig. 2 we also show error bars from variations of both MSTW and NN pdf error sets. It is striking that uncertainty estimates of the NN pdfs are significantly larger than the ones from MSTW, reaching a similar size to the scale variation band. Nevertheless, the central values agree well. The difference between top and anti-top rapidities is sensitive to the top quark charge asymmetry at the LHC. We find similar uncertainties as for the rapidity distribution. However, here, NLO effects introduce significant shape changes with respect to the LO, as can be seen from the differential K-factor in the lower pane of the plot.

Increasing the LHC center of mass energy from 14 TeV to 33 TeV increases the total $t\bar{t}$ cross section by a factor of 6 to almost 5 nb. The residual scale uncertainty is 11%, similar to the 14 TeV case. Uncertainties from pdfs are expected to be larger since the gluon large- x pdfs is only weakly constrained. The K-factor is notably smaller at $K = 1.23$.

3 Boosted kinematics

In this section we summarize theoretical uncertainties of the previously presented observables in the boosted regime at the 14 TeV LHC. In particular, we require that p_{\perp}^t or $p_{\perp}^{\bar{t}} \geq 600$ GeV. The NLO $t\bar{t}$ cross section is 1.05 pb [3], about 800 times smaller than the total NLO cross section. Scale variations by a factor of two around a central scale of $\mu_0 = 600$ GeV give an uncertainty of 15%, similar to the total NLO cross section. Error bands of MSTW pdfs are about 10%, twice as big as compared to the total cross section. In Fig. 3, we show transverse momentum and rapidity distribution and their uncertainties for p_{\perp}^t or $p_{\perp}^{\bar{t}} \geq 600$ GeV. The error bars of single histogram bins range up to 20-30%. NLO QCD corrections induce moderate

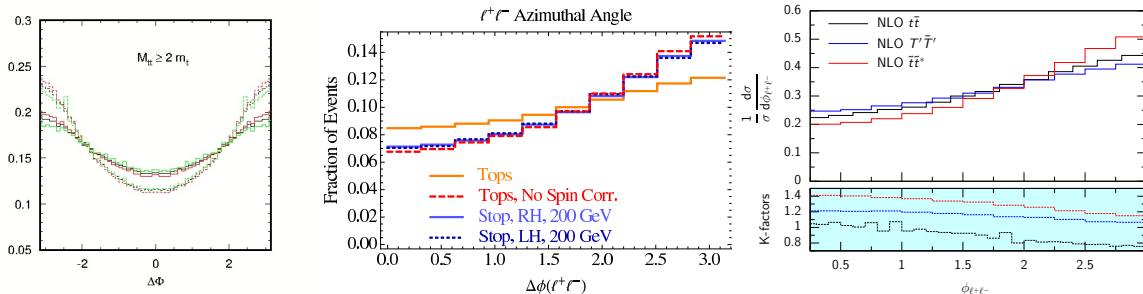


Figure 3: Distributions of the dilepton azimuth angle from Refs. [30, 24, 26], respectively. Fig. (a) shows spin correlated (solid) and spin uncorrelated (dashed) top quarks. The hatched area around the solid lines corresponds to scale variations. Fig. (b) compares SM $t\bar{t}$ spin correlations with 200 GeV stop quarks decaying into a massless neutralino and a top quark. In (c) NLO QCD predictions are shown for SM $t\bar{t}$ (black), fermionic partners of mass 500 GeV (blue) and scalar partners of mass 250 GeV (red). The corresponding K-factors are shown in the lower pane.

shape changes but the overall K-factor of 1.45 is 10% larger than for the total cross section.

It is interesting to note that the calculations of Refs. [17, 18] indicate that soft-gluon effects can be important at high energies. In particular, Ref. [17] considers the p_{\perp} distribution and finds corrections of up to 100% wrt. NLO results for highly boosted top quarks. Similarly, the authors of Ref. [18] calculate the soft plus virtual approximation to NNLO QCD correction of the $t\bar{t}$ invariant mass distribution and come to similar conclusions. For example, at $m_{t\bar{t}} = 1.5$ TeV their approximate NNLO corrections exceeds the size of the corresponding NLO QCD correction. These results are in apparent tension with the $\mathcal{O}(15 - 30\%)$ uncertainty estimates obtained in NLO QCD calculations, and further work will be required to resolve this point.

The effects of weak virtual corrections in $t\bar{t}$ production have been studied e.g. in Ref. [19] (see also references therein). Effects on the total cross section are small, at 2% for LHC energies of 14 TeV and 33 TeV. The corrections can be significantly larger in the tail of energy-related differential distributions. As shown in Ref. [19], at transverse momenta $p_{\perp}^t \approx 1$ TeV weak virtual corrections are -10% with respect to the LO prediction, and they grow to -18% at $p_{\perp}^t \approx 2$ TeV. Similarly at invariant masses of $m_{t\bar{t}} \approx 2$ TeV the corrections amount to -6% . Effects of partial cancellations between these weak virtual corrections with the corresponding emission of collinear Z and W bosons has been studied in Ref. [20]. It was found that at $p_{\perp}^t = 500$ GeV the cancellation is 1-2%. At higher energies $p_{\perp}^t \approx 1$ TeV the cancellation can become larger, but the details of acceptance cuts may significantly affect the relative importance of the weak boson emission processes.

4 Top quark spin correlations

Top quark spin correlations are a unique tool for studying the interplay between electroweak and strong physics in the top quark sector. After the evidence of top quark spin correlations at the Tevatron [21] and recently the observation at the LHC [22, 23], experimental analyses

will soon be able to probe the effects of New Physics models on SM spin correlations.

The cleanest $t\bar{t}$ samples are the ones with two opposite sign leptons in the final state. Spin correlations in this di-leptonic decay mode manifest themselves most prominently in the angle between the two leptons. In fact, the azimuthal opening angle has been shown to be most robust under higher order corrections and parton showering effects. The effects of higher order corrections have been studied e.g. in Refs. [9, 10]. For standard acceptance cuts, NLO QCD effects introduce shape changes of at most 20%. If additional cuts are applied that enhance spin correlations, NLO corrections increase the correlation even further. Electroweak corrections have negligible effects, and scale variations are vanishingly small because distributions are typically normalized (see Fig. 4 a). On the experimental side, the reconstruction of the lepton opening angle in the laboratory frame does not involve the kinematics of other particles and can therefore be extracted with small systematic uncertainties. The normalized azimuthal opening angle distribution is therefore an ideal observable for studying top quark spin correlations. Of course, other constructions such as helicity angles, double differential distributions, and asymmetries can also be explored.

It has been shown that top quark spin correlations can be used to distinguish SM top quarks from scalar or fermionic partners. For example, using spin correlations alone light stop quarks of $m_{\tilde{t}} = 200$ GeV can be excluded at 95% C.L. using 20 fb^{-1} at the 8 TeV LHC [24]. It is also possible to use spin correlations for distinguishing heavy fermionic top partners from scalar partners. It has been pointed out [25, 26] that QCD corrections play an important role in correctly understanding these processes. In fact, for the pair production of light scalar top partners with $m_{\tilde{t}} \leq 300$ GeV and heavy fermion partners with $m_{T'} \geq 500$ GeV (decaying into $t\bar{t}$ final states plus large missing energy), significantly different NLO K -factors can result in approximately equal cross sections $\sigma_{t\bar{t}^*}^{\text{NLO}} \approx \sigma_{TT'}^{\text{NLO}}$. Spin correlations, however, show significantly different shapes and help to separate the two hypotheses. Fig. 4 c shows an example for the processes $pp \rightarrow \tilde{t}\tilde{t}^*(m_{\tilde{t}} = 250 \text{ GeV}) \rightarrow t\bar{t} + \chi^0\chi^0(m_{\chi^0} = 50 \text{ GeV})$ and $pp \rightarrow T\bar{T}'(m_{\tilde{t}} = 500 \text{ GeV}) \rightarrow t\bar{t} + A^0A^0(m_{\chi^0} = 50 \text{ GeV})$. It should be noted that NLO K -factors (lower pane of Fig. 4 c) are similar in size to the separation between SM $t\bar{t}$ production and the BSM signals, emphasizing the importance of higher order effects for these processes.

In the event of a discovery of a new resonance which decays into $t\bar{t}$ pairs, top quark spin correlations can also be used to analyze the couplings of this new particle [27, 28]. Another interesting aspect are New Physics contributions to the top quark chromomagnetic $\hat{\mu}_t$ and electric \hat{d}_t dipole moments. Refs. [29, 30] demonstrate that New Physics contributions to $\hat{\mu}_t$ and \hat{d}_t can be exposed through spin correlations in the di-leptonic and in the semi-leptonic decay mode. From the dileptonic sample of the 20 fb^{-1} run at 8 TeV, it should be possible to constrain $\text{Re } \hat{\mu}_t$ and $\text{Re } \hat{d}_t$ at the few percent level. The imaginary parts $\text{Im } \hat{\mu}_t$ and $\text{Im } \hat{d}_t$ can be constrained from lepton-top helicity angles in the semi-leptonic channel where a full reconstruction of the $t\bar{t}$ system is possible. Using the same dataset limits of about 15-20% are possible. Ref. [29] finds that constraints of 1% or below are possible with 100 fb^{-1} at 13 TeV.

5 Inclusive Top Quark Charge Asymmetry at LHC 14

Here we detail some estimates toward the measurability of the SM forward-backward asymmetry A_{FC} at the 14 TeV LHC. The increased center of mass energy, relative to LHC 7 and LHC 8, increases the proportion of $t\bar{t}$ events that arise from (symmetric) gluon fusion, so the size of the signal decreases with increasing center of mass energy. As we will demonstrate below, the observability of the SM asymmetry at LHC 14 depends sensitively on the evolution of experimental systematic uncertainties, and we will discuss prospects and scenarios for their improvement.

Already at LHC 7, measurements of the top forward-central asymmetry are systematically limited. Current LHC measurements in the lepton+jets channel are done with the full 5 fb^{-1} 7 TeV dataset. CMS finds [31]

$$A_{FC} = 0.004 \pm 0.010 \pm 0.011. \quad (1)$$

ATLAS, in their similar study, marginalizes over sources of systematic uncertainty according to a novel procedure [32] and claims [33]

$$A_{FC} = 0.006 \pm 0.010 \quad (2)$$

where the quoted uncertainty is now almost entirely statistical in origin. Prior to the marginalization, the individual systematic uncertainties tabulated in Table 3 of Ref. [33] add in quadrature to a total systematic uncertainty comparable to that of CMS' result. Without this marginalization procedure, the systematic uncertainty on the current measurements of A_{FC} is comparable to the size of the predicted SM effect [34],

$$A_{FC} = 0.0123 \pm 0.0005 \quad (3)$$

at LHC 7.

SM predictions for LHC 14 as a function of cuts on minimum top pair invariant mass $m_{t\bar{t}}$ or velocity $\beta_{t\bar{t}}$ are calculated in Ref. [34] and shown in Fig. 5. Specifically, we use predictions for the quantity

$$A_{FC}^\eta = \frac{N(\Delta|\eta| > 0) - N(\Delta|\eta| < 0)}{N(\Delta|\eta| > 0) + N(\Delta|\eta| < 0)} \quad (4)$$

where $\Delta|\eta| \equiv |\eta_t| - |\eta_{\bar{t}}|$ looks at whether the reconstructed top or anti-top is more central according to lab-frame *pseudo-rapidity*. Cutting on either CM invariant mass or CM rapidity increases the proportion of $q\bar{q}$ -initiated top pair events relative to gluon-initiated events, and thus enhances the signal. It can be seen from Fig. 5, however, that even after imposing kinematic cuts, the size of the signal at the 14 TeV LHC is comparable to the systematic uncertainties on the current measurements. Unlike at the 7 TeV LHC, statistical uncertainties will not be limiting given current projections for the integrated luminosities to be achieved at 14 TeV.

The dominant contributions to the experimental systematics are collected in Table 1. Several systematic uncertainties arise from uncertainties associated with the nature of the measurement of the forward charge asymmetry, as well as assumptions in background and top

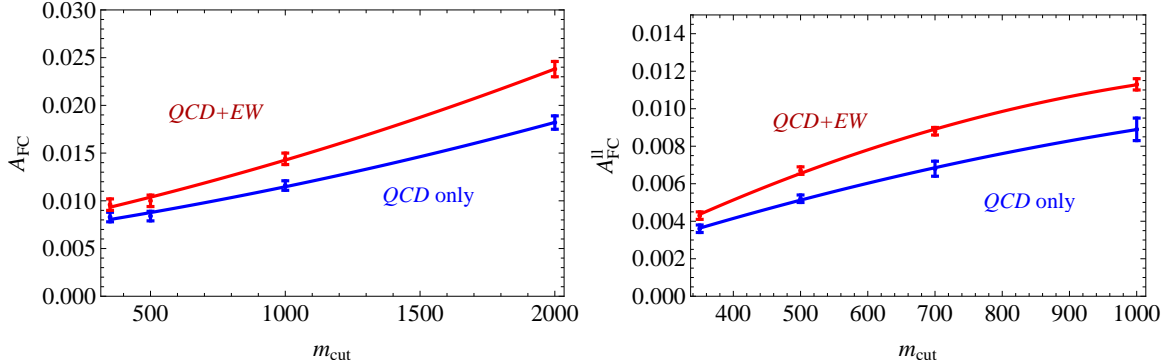


Figure 4: Inclusive NLO SM predictions for the top quark asymmetry (left) and *inclusive* lepton asymmetry (right) as a function of minimum CM invariant mass. Points with error bars are results calculated in Ref. [34], showing the theoretical uncertainty arising from scale variation; the curves are interpolations used in the present study. Incorporating standard acceptance cuts on the leptons reduces the lepton asymmetry by more than a factor of two.

quark modeling. Each uncertainty is treated in its own way, but the common technique for A_{FC} is to compare a measurement using a baseline model with one where one of the inputs has been varied within its known error.

Systematic uncertainties taken into account in measurements of A_{FC} include those from detector effects (such as jet energy scale/resolution, lepton energy scale/resolution, and pileup), modeling uncertainties (such as MC generator and hadronization, MC-derived backgrounds, and PDF uncertainties), and uncertainties from measurement techniques (such as unfolding). The leading two systematics in each measurement are either simulation modeling uncertainties or calibration uncertainties for leptons and jets. These uncertainties will not necessarily scale with integrated luminosity without improvements in technique. Jet energy and lepton energy scale, which are derived from comparisons between data and Monte Carlo, could possibly be reduced in a larger dataset, though uncertainties are currently dominated by disagreement between Monte Carlo generators. Moreover, any increased pileup will likely contribute to increasing the overall uncertainty. However, jet and lepton energy scale uncertainties are already small enough to allow a significant measurement of $A_{FC} > 0.01$ in the semi-leptonic channel if $t\bar{t}$ modeling uncertainties can be significantly reduced, at least by half. One approach to reducing the limiting modeling uncertainties has already been advanced by ATLAS in their most recent semi-leptonic measurement [33].

Additionally, combining measurements across experiment and channel will further reduce uncorrelated uncertainties, allowing for reductions in the overall systematic uncertainty. Given that systematic uncertainties on A_{FC} are already on the order of 0.01, it is certainly reasonable to assume that a significant measurement of the SM forward charge asymmetry will be possible at LHC 14, and will grow in significance for physics beyond the Standard Model which predicts an enhancement. However, it will largely be improvements in modeling techniques that will allow this, not increased integrated luminosity, and no further benefit is obtained at the HL-LHC.

We present three scenarios for potential improvement of systematic uncertainties to show

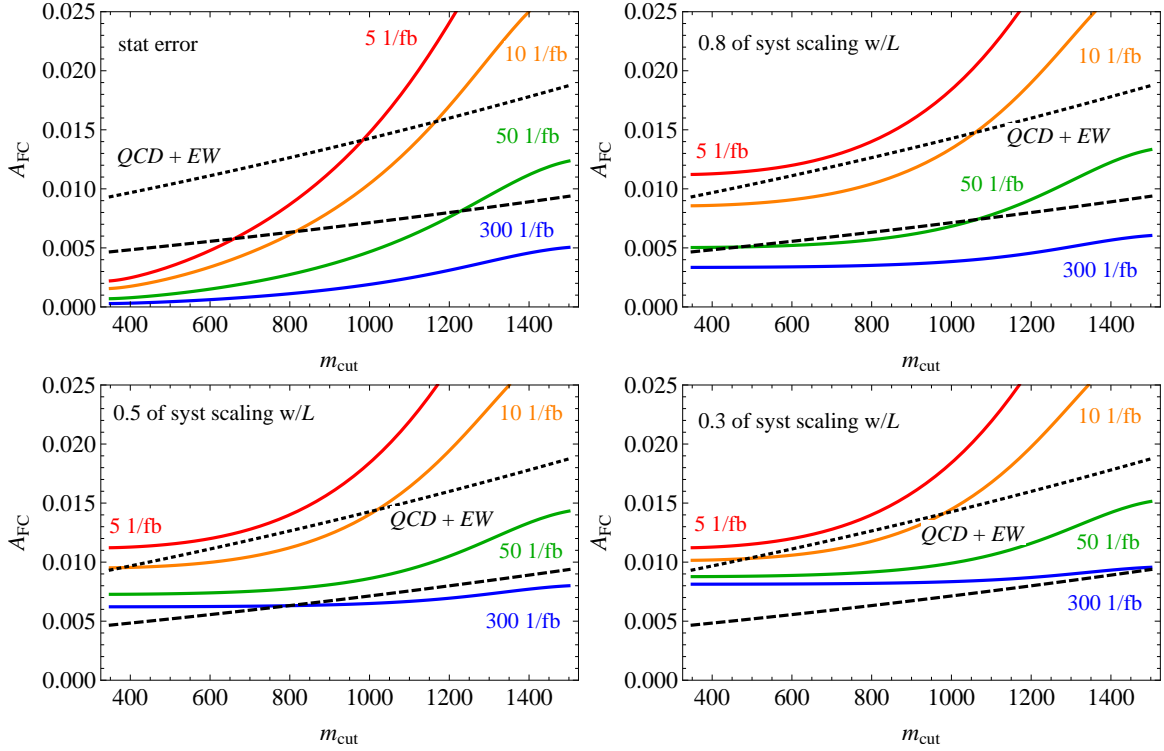


Figure 5: SM asymmetry compared to projected uncertainty on the measurement in the lepton+jet channel at LHC 14, as a function of minimum $m_{t\bar{t}}$, with three different scenarios for the improvement of systematic uncertainties with luminosity. The dotted line shows the SM (QCD and EW combined) predictions of Ref. [34], and the dashed line shows $0.5 \times$ the asymmetry to indicate 95% CL sensitivity. Top left: statistical error only. Top right: statistical error combined in quadrature with systematic error given by Eq. 1 at 5 fb⁻¹, with 0.8 of the systematic uncertainty scaling as $1/\sqrt{\mathcal{L}}$. Bottom left: statistical error combined in quadrature with systematic error given by Eq. 1 at 5 fb⁻¹, 0.5 of which scales as $1/\sqrt{\mathcal{L}}$. Bottom right: statistical error combined in quadrature with systematic error given by Eq. 1 at 5 fb⁻¹, 0.3 of which scales as $1/\sqrt{\mathcal{L}}$.

Experiment	Channel	Leading Systematic	Second Leading Systematic
ATLAS	Semi-leptonic	Jet energy scale 0.003	Lepton energy scale 0.003
	Dileptonic	$t\bar{t}$ model dependence 0.015	Multi-jet modeling 0.012
CMS	Semi-leptonic	$t\bar{t}$ model dependence 0.007	Lepton energy scale 0.006
	Dileptonic	Migration matrix (+Sys.) +0.01	$t\bar{t}$ model dependence (-Sys) -0.03

Table 1: Measurements of A_{FC} using approximately 5 fb^{-1} of 7 TeV data at CMS and ATLAS for both $t\bar{t}$ decay channels. The two largest systematics are shown along with their respective magnitudes. Note that the dilepton measurement at ATLAS evaluates systematics separately for each lepton channel and combines them to reduce the overall systematic uncertainty; the listed systematic uncertainties are for the electron-electron channel. The migration matrix uncertainty, as listed in the CMS dilepton measurement, is due to the finite Monte Carlo statistics used in the response matrix of an unfolding technique.

the sensitivity range at LHC 14 that results. In Fig. 5 we plot statistical and combined statistical+systematic uncertainties on A_{FC} at LHC 14. Statistical errors are shown assuming semi-leptonic top pair decays with an approximate (flat) efficiency for top identification and reconstruction of $\epsilon = 0.2$ per (semi-leptonic) event. This efficiency represents the requirement that at least one (isolated) lepton and at least 4 jets lie within $|\eta| < 2.4$, with $p_{T,j} > 30$ GeV, $p_{T,e} > 30$ GeV, and $p_{T,\mu} > 20$ GeV, with the further requirement that solving quadratic equations for the missing neutrino four-momentum yield a physical solution. The cross-section is normalized to a NLO prediction of 845 pb using a constant K-factor. In all cases we take the systematic uncertainty at 5 fb^{-1} to be given by the systematic uncertainty reported by CMS with 5 fb^{-1} of LHC 7 data, and then evolve the systematic uncertainties with luminosity assuming a fraction (0.3, 0.5, 0.8) of the systematic uncertainty scales as $1/\sqrt{\mathcal{L}}$. Based on this estimate, with sufficient luminosity, LHC14 will have sensitivity to the SM asymmetry if at least 0.5 of the systematic errors scale with luminosity. Optimistic scenarios involving significant improvement in modeling techniques would more closely resemble the “statistical only” cases, and would have excellent prospects with much less luminosity.

5.1 Leptonic charge asymmetry

The dileptonic channel offers another window into top pair production asymmetries, albeit at smaller statistics due to the reduced branching fraction. Current LHC measurements in the dileptonic channel are done at 7 TeV and have, with 5 fb^{-1} , comparable systematic errors to those in the semileptonic channel [35, 36]. An alternate possibility in the dileptonic channel is to measure an asymmetry of the leptons rather than of the tops themselves,

$$A_{\ell\ell} = \frac{N(\Delta|\eta_\ell| > 0) - N(\Delta|\eta_\ell| < 0)}{N(\Delta|\eta_\ell| > 0) + N(\Delta|\eta_\ell| < 0)}, \quad (5)$$

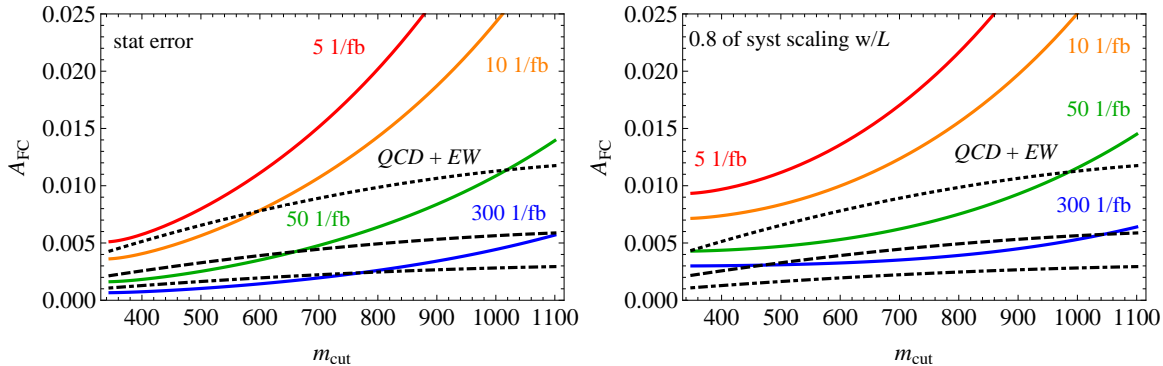


Figure 6: SM inclusive lepton asymmetry compared to projected uncertainty on the measurement at LHC 14, as a function of minimum $m_{t\bar{t}}$, with and without systematic uncertainties. The dotted line shows the SM (QCD and EW combined) predictions of Ref. [34], the dashed line shows $0.5 \times$ the asymmetry, and the dash-dotted line shows 0.25 the asymmetry to give a rough estimate of 95% CL sensitivity recalling the washout due to finite lepton acceptance cuts. Left: statistical error only. Right: statistical error combined in quadrature with systematic error given by $\Delta A = 0.007$ at 5 fb^{-1} , with 0.8 of the systematic uncertainty scaling as $1/\sqrt{\mathcal{L}}$.

where $\Delta|\eta_\ell| \equiv |\eta_{\ell^+}| - |\eta_{\ell^-}|$. The systematic uncertainty quoted in the measurement of this leptonic asymmetry is smaller than the uncertainty on the parent top asymmetry, 0.6% in CMS [36] and 0.8% in ATLAS [35]. However, the asymmetry itself is also smaller, especially when realistic geometric acceptance cuts are taken into account. We emphasize that including standard acceptance cuts decreases the size of the lepton asymmetry by more than a factor of two [34].

To estimate the reach in the leptonic asymmetry we use an approximate (flat) efficiency for top pair identification and reconstruction of $\epsilon = 0.25$ per dileptonic top pair event, again accounting for geometric and p_T acceptance and an additional finite efficiency for reconstructing the top pair from the measured missing momentum. Results are shown in Fig. 5.1. Observation of the SM effect in this channel does not look promising; the reduction in the systematic error bars is more than compensated by the intrinsically smaller signal.

6 New observables for the top charge asymmetry at the LHC

In contrast to A_{FC} in $t\bar{t}$ production, the asymmetry in $t\bar{t} + j$ final states has the advantage that it is non-vanishing at LO and NLO calculations are available [37, 38, 39, 40, 41, 42]. It was found that higher order corrections in the production and in the decay process reduce the LO asymmetry A_{FB} at the Tevatron. Refs. [39, 42] provide arguments for these effects which should also hold for A_{FC} at the LHC. Ref. [43] introduces two new observables to access the production-level asymmetries in $t\bar{t} + j$ events. First, the *incline asymmetry* measures the asymmetry in the relative angle between the decay plane (i.e., that containing the t , \bar{t} and jet),

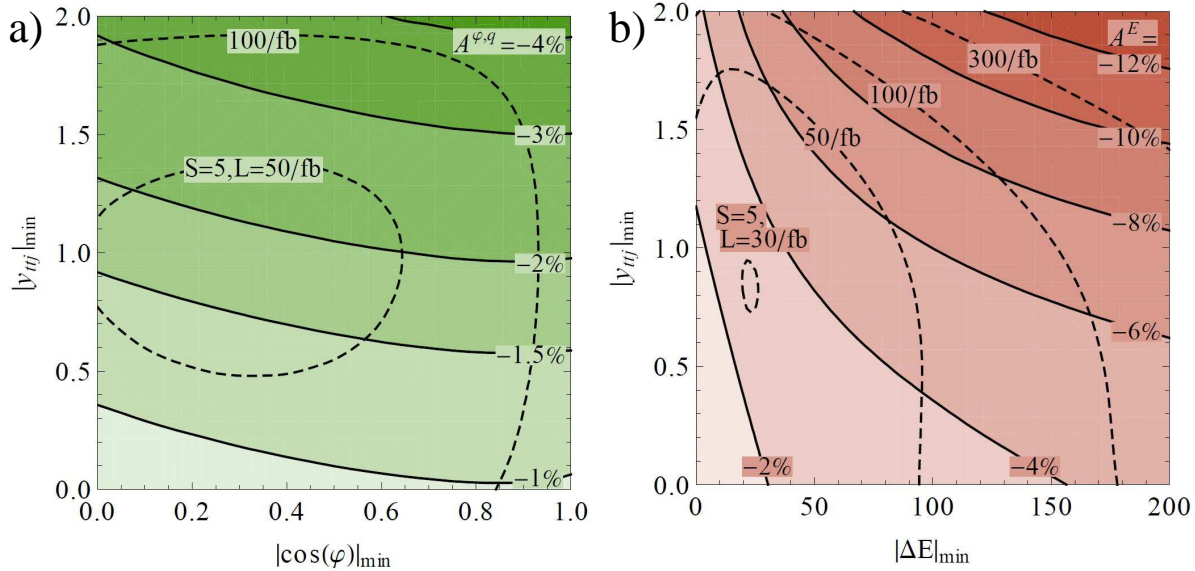


Figure 7: Observability contours of asymmetry variables in $t\bar{t}$ +jet final states at LHC14, as a function of cuts on $t\bar{t}$ +jet events. Left: the incline asymmetry as a function of the minimum required incline angle and the minimal required system rapidity $|y_{t\bar{t}j}|$. Right: the energy asymmetry as a function of the minimum required energy difference and the minimal required system rapidity. Further details are available in Ref. [43, 2].

and the production plane (i.e., that defined by the jet and the incoming partons). Second, the *energy asymmetry* between the t and \bar{t} energies is particularly useful for probing asymmetries in qg -initiated events. A Snowmass 2013 study for these variables was carried out in [2], and the results are briefly summarized here.

In $t\bar{t} + j$ events, the incline asymmetry (as opposed to the forward-central asymmetry) benefits from the additional information provided by the $t\bar{t} + j$ event kinematics. Ref. [43] finds that it is possible to measure an incline asymmetry of the order of 4% with a significance of three standard deviations with 100 fb^{-1} at 14 TeV (see Fig. 6).

Extrapolating this to 3000 fb^{-1} of integrated luminosity yields a significance of about 16 s.d. for both observables. Calculations carried out for the new observables are currently performed at leading order, and NLO corrections to the new observables could be sizeable, thus affecting the projected sensitivities.

Because of the decreasing fraction of $q\bar{q}$ -initiated events with increasing center-of-mass energies, a measurement at 100 TeV would require extremely strong cuts to suppress the gg initial state contributions. For reasonably large asymmetries of around 8% wide $|y|$, cuts of up to 5 are needed for the rapidity of the $t\bar{t} + j$ system [2].

6.1 Asymmetry at LHCb

Measurement of a top-antitop rate asymmetry at the LHCb experiment could provide further information on the top quark asymmetry [44]. LHCb has unique capabilities to measure the charge asymmetry in top quark production. An official LHCb study was performed for

Snowmass 2013 [1] and the results are briefly summarized here.

In top quark production at LHCb, as at ATLAS and CMS, the best reach is provided by the lepton+jets decay channel, although the dileptonic decay channel can provide supplementary reach. Table 2 summarizes cross sections as predicted by POWHEG within the LHCb acceptance. The uncertainties are estimated from scale variations, comparing the central PDF sets from different groups (CTEQ, MSTW, NNPDF) and shower as well as tagging uncertainties. Despite lower backgrounds in the dilepton final state, the production yield at LHCb makes measurements in the dilepton decay channel not statistically significant, although the high luminosity phase of the LHC may offer enough integrated luminosity to change this conclusion.

Channel	σ (fb) at 8 TeV	σ (fb) at 14 TeV
lb	675 ± 110	5353 ± 780
lbj	254 ± 41	2758 ± 410
lbb	111 ± 22	1296 ± 233
$lbbj$	68 ± 13	860 ± 156
ll	79 ± 15	635 ± 109
llb	19 ± 4	417 ± 79

Table 2: Summary of $t\bar{t}$ inclusive cross section channels within LHCb acceptance for LHC8 and LHC14. The predicted cross sections are computed with a 60 GeV cut for the transverse momentum of the leading b jet.

The large pseudorapidity coverage at LHCb allows differential charge asymmetry measurements to be made in the forward region. Here on one hand the intrinsic size of the asymmetry is enhanced, and on the other hand, the dominant asymmetric background from W +jet production is reduced. The study [1] concludes that with enough (expected integrated luminosity after LS1 is 50 fb^{-1}) integrated luminosity at 14 TeV a measurement of the charge asymmetry in top quark production at the LHCb can be done. The high luminosity phase of the 14 TeV LHC makes it possible to also measure the charge asymmetry in the dilepton decay channel. No degradation due to pile-up effects is anticipated, allowing unchanged trigger settings with respect to current 7 and 8 TeV running conditions. Measurements from LHCb are complementary to the measurements in the central region performed by ATLAS and CMS and thus contribute to a deeper understanding of top quark production. A combination of LHCb results with those from ATLAS and CMS would shed further light into the top charge asymmetry puzzle.

7 Conclusions

We have presented an overview of the theoretical understanding of top quark pair production, presenting a unified study of uncertainties in top kinematic distributions and surveying

prospects for and uncertainties in top spin correlations. LHC 14 has good prospects for resolving outstanding questions in boosted top production cross-sections and production asymmetries. Good control of systematic uncertainties is necessary to decisively measure a SM-like top pair production asymmetry at LHC 14, but other, less inclusive observables, such as the incline asymmetry of Ref. [43] or the forward rate asymmetry at LHCb, are less limited by systematic uncertainties.

Acknowledgements. We acknowledge useful conversations with Thorsten Chwalek and Frederic Deliot regarding sources of systematic errors. MS is supported by US DOE under contract DE-AC02-06CH11357. JS is supported by NSF grant PHY-1067976 and the LHC Theory Initiative under grant NSF-PHY-0969510.

References

- [1] R. Gauld, LHCb-PUB-2013-009; CERN-LHCb-PUB-2013-009 (2013)
- [2] S. Berge and S. Westhoff, arXiv:1307.6225 [hep-ph].
- [3] J. M. Campbell and R. K. Ellis, Nucl. Phys. Proc. Suppl. **205-206**, 10 (2010) [arXiv:1007.3492 [hep-ph]].
- [4] W. Bernreuther, A. Brandenburg, Z. G. Si and P. Uwer, Phys. Rev. Lett. **87**, 242002 (2001) [hep-ph/0107086].
- [5] W. Bernreuther, A. Brandenburg, Z. G. Si and P. Uwer, Nucl. Phys. B **690**, 81 (2004) [hep-ph/0403035].
- [6] S. Frixione and B. R. Webber, hep-ph/0612272.
- [7] S. Frixione, P. Nason and G. Ridolfi, JHEP **0709**, 126 (2007) [arXiv:0707.3088 [hep-ph]].
- [8] S. Frixione, P. Nason and G. Ridolfi, arXiv:0707.3081 [hep-ph].
- [9] K. Melnikov and M. Schulze, JHEP **0908**, 049 (2009) [arXiv:0907.3090 [hep-ph]].
- [10] W. Bernreuther and Z. -G. Si, Nucl. Phys. B **837**, 90 (2010) [arXiv:1003.3926 [hep-ph]].
- [11] A. Denner, S. Dittmaier, S. Kallweit and S. Pozzorini, Phys. Rev. Lett. **106**, 052001 (2011) [arXiv:1012.3975 [hep-ph]].
- [12] G. Bevilacqua, M. Czakon, A. van Hameren, C. G. Papadopoulos and M. Worek, JHEP **1102**, 083 (2011) [arXiv:1012.4230 [hep-ph]].
- [13] J. M. Campbell and R. K. Ellis, arXiv:1204.1513 [hep-ph].
- [14] A. Denner, S. Dittmaier, S. Kallweit and S. Pozzorini, JHEP **1210**, 110 (2012) [arXiv:1207.5018 [hep-ph]].

- [15] A. D. Martin, W. J. Stirling, R. S. Thorne and G. Watt, *Eur. Phys. J. C* **63**, 189 (2009) [arXiv:0901.0002 [hep-ph]].
- [16] R. D. Ball, V. Bertone, S. Carrazza, C. S. Deans, L. Del Debbio, S. Forte, A. Guffanti and N. P. Hartland *et al.*, *Nucl. Phys. B* **867**, 244 (2013) [arXiv:1207.1303 [hep-ph]].
- [17] B. Auerbach, S. V. Chekanov and N. Kidonakis, arXiv:1301.5810 [hep-ph].
- [18] A. Ferroglia, B. D. Pecjak and L. L. Yang, arXiv:1306.1537 [hep-ph].
- [19] J. H. Kühn, A. Scharf and P. Uwer, arXiv:1305.5773 [hep-ph].
- [20] U. Baur, *Phys. Rev. D* **75**, 013005 (2007) [hep-ph/0611241].
- [21] V. M. Abazov *et al.* [D0 Collaboration], *Phys. Rev. Lett.* **108**, 032004 (2012) [arXiv:1110.4194 [hep-ex]].
- [22] G. Aad *et al.* [ATLAS Collaboration], *Phys. Rev. Lett.* **108**, 212001 (2012) [arXiv:1203.4081 [hep-ex]].
- [23] [CMS Collaboration], report CMS-PAS TOP-12-004.
- [24] Z. Han, A. Katz, D. Krohn and M. Reece, *JHEP* **1208**, 083 (2012) [arXiv:1205.5808 [hep-ph]].
- [25] R. Boughezal and M. Schulze, arXiv:1212.0898 [hep-ph].
- [26] R. Boughezal and M. Schulze, in preparation.
- [27] M. Baumgart and B. Tweedie, *JHEP* **1109**, 049 (2011) [arXiv:1104.2043 [hep-ph]].
- [28] F. Caola, K. Melnikov and M. Schulze, *Phys. Rev. D* **87**, 034015 (2013) [arXiv:1211.6387 [hep-ph]].
- [29] M. Baumgart and B. Tweedie, *JHEP* **1303**, 117 (2013) [arXiv:1212.4888 [hep-ph]].
- [30] W. Bernreuther and Z. -G. Si, arXiv:1305.2066 [hep-ph].
- [31] S. Chatrchyan *et al.* [CMS Collaboration], *Phys. Lett. B* **717**, 129 (2012) [arXiv:1207.0065 [hep-ex]].
- [32] G. Choudalakis, arXiv:1201.4612 [physics.data-an].
- [33] G. Aad *et al.* [ATLAS Collaboration], ATLAS-CONF-2013-078.
- [34] W. Bernreuther and Z. -G. Si, *Phys. Rev. D* **86**, 034026 (2012) [arXiv:1205.6580 [hep-ph]].
- [35] [ATLAS Collaboration], ATLAS-CONF-2012-057.
- [36] [CMS Collaboration], CMS-PAS-TOP-12-010.

- [37] S. Dittmaier, P. Uwer and S. Weinzierl, *Eur. Phys. J. C* **59**, 625 (2009) [arXiv:0810.0452 [hep-ph]].
- [38] G. Bevilacqua, M. Czakon, C. G. Papadopoulos and M. Worek, *Phys. Rev. Lett.* **104**, 162002 (2010) [arXiv:1002.4009 [hep-ph]].
- [39] K. Melnikov and M. Schulze, *Nucl. Phys. B* **840**, 129 (2010) [arXiv:1004.3284 [hep-ph]].
- [40] A. Kardos, C. Papadopoulos and Z. Trocsanyi, *Phys. Lett. B* **705**, 76 (2011) [arXiv:1101.2672 [hep-ph]].
- [41] S. Alioli, S. -O. Moch and P. Uwer, *JHEP* **1201**, 137 (2012) [arXiv:1110.5251 [hep-ph]].
- [42] K. Melnikov, A. Scharf and M. Schulze, *Phys. Rev. D* **85**, 054002 (2012) [arXiv:1111.4991 [hep-ph]].
- [43] S. Berge and S. Westhoff [arXiv:1305.3272 [hep-ph]].
- [44] A. L. Kagan, J. F. Kamenik, G. Perez, S. Stone *Phys. Rev. Lett.* **107**, 082003 (2011) [arXiv:1103.3747 [hep-ph]].